Phase diagrams of magnetically disordered bilayers

Marcelo L. Lyra and Crisógono R. da Silva
Departamento de Física, Universidade Federal de Alagoas, 57061 Maceió, Alagoas, Brazil
(Received 22 November 1991; revised manuscript received 23 March 1992)

The phase diagrams of magnetically coupled bilayer models composed of two Bethe lattices are exactly evaluated using the partial-partition-function technique. Special attention is devoted to disordered systems in the limit of annealed bond distribution. Correlations between bonds localized in different layers lead to very interesting features. A new percolation threshold in the intralayer-dilution limit is exactly obtained for n-coupled Bethe and square lattices. As competing intralayer parameters are considered, a multiple reentrant behavior appears, which is related to the relative role played by thermal fluctuations on frustration, bond-bond, and spin-spin correlations.

INTRODUCTION

The interest in the understanding of the main behavior of magnetically coupled layers has recently increased because of the quick developments in the technology of preparing high-quality thin films, such as magnetic overlayers, sandwiches, and superlattices.[1] These systems display a great variety of unusual properties. For example, magnetism in the substrate as well as dead layers in the overlayer may be induced by interfacial couplings.[2] Coupling through nonmagnetic layers shows oscillatory behavior and can lead to giant magnetoresistance,[3] while ferromagnetically coupled superlattices can have new spin-wave dispersion branches stabilized as a result of induced periodicities.[4] Such effects, which also involve the critical[5] and dynamical[6] aspects, suggest a profusion of new applications.

Lately, a good deal of work on coupled superconducting layers has been developed.[7] There is a close relation, evidenced by experimental and theoretical works, between the high-T_c superconductivity and the magnetic interactions on the layers of CuO_2 (Ref. 8) commonly present in most superconducting ceramics. The disorder and competition effects introduced by mobile holes in the oxygen band play a fundamental role in the Cooper-pairing mechanism.[9] Also, it is observed in Tl compounds that the superconducting transition temperature increases with the number of interacting CuO_2 planes.[10] Although such increase is believed to be related to a quantum-well-confinement effect,[11] a careful analysis of the magnetic behavior of coupled disordered layers, especially their magnetic phase diagram, is clearly desirable to improve our knowledge of the behavior and properties of such systems.

In this work we determine the phase diagram of a coupled bilayer model with intralayer and interlayer disorder, in the regime of annealed bond distribution. The annealing procedure allows the bonds to move in order to minimize globally the Helmholtz free energy. The annealing induces statistical bond-bond correlations, so that their distribution is not random at all. These correlations lead to very interesting features in the phase diagram as a new percolation threshold in the intralayer dilution limit and a phenomenon of multiple reentrance when competing interactions are introduced.

We will consider a bilayer structure composed of two coupled Bethe lattices with coordination number $q+1$. The Bethe-lattice approach is known to describe the general features of models with competing interactions and disorder.[12] Our model is exactly solved by means of a generalization of the method of partial partition functions commonly used in Bethe-lattice approaches.[13] Although a Bethe-lattice approach predicts higher transition temperatures when compared with more realistic systems, we believe that it correctly gives the general shape of the phase diagram.

COUPLED BETHE LATTICES: FORMALISM AND PHASE DIAGRAM

A bilayer Bethe lattice is constructed by connecting to a central interacting pair of sites $q+1$ pairs in order to constitute the first generation. The construction of the successive generations is performed by connecting q pairs to each pair of the previous generation. A similar procedure has been recently performed to study the spin-glass transition in a Bethe lattice in which a coupling between replicas was considered.[14] In our basic model we assign to each site an Ising spin which interacts through an exchange interaction with coupling constant J with their nearest neighbors localized in the same layer and also through an exchange-interaction coupling constant γJ with the corresponding one in the adjacent layer. The Hamiltonian for this model can be written as

$$H=-J\sum_{i,j}(\sigma_i^1\sigma_j^1+\sigma_i^2\sigma_j^2)-\gamma J\sum_i\sigma_i^1\sigma_i^2\ , \tag{1}$$

where σ_k^l represents the spin localized at site k of layer l and the first sum runs over all nearest-neighbor intralayer

pairs. The exact partition function for a tree with $N+1$ generations can be written as

$$Z_{N+1}=\sum_{\sigma_0^1,\sigma_0^2} Z_{N+1}(\sigma_0^1,\sigma_0^2)\ , \tag{2}$$

where $Z_{N+1}(\sigma_0^1,\sigma_0^2)$ is the partial partition function for a particular configuration of the central pair. Each partial partition function is recursively obtained in terms of the partition functions of connected branches through the relation

$$Z_{N+1}(\sigma_0^1,\sigma_0^2)=\exp(\gamma K\sigma_0^1\sigma_0^2)\prod_{i=1}^{q+1}\sum_{\sigma_i^1,\sigma_i^2}\exp[K(\sigma_0^1\sigma_i^1+\sigma_0^2\sigma_i^2)]Z_N(\sigma_i^1,\sigma_i^2)\ , \tag{3}$$

where $K=J/k_BT$. A quite similar recursion relation is obtained for the partial partition functions of successive branches where the product is made only over the q external pairs. The four recursion relations given by Eq. (3), after summing up the pair configurations, can be reduced to a system of three relations in terms of appropriated effective fields:

$$\begin{aligned}\exp[2X_{N+1}]&=\frac{Z_{N+1}(+,+)}{Z_{N+1}(-,-)}\ ,\\ \exp[2Y_{N+1}]&=\frac{Z_{N+1}(+,-)}{Z_{N+1}(-,-)}\ ,\\ \exp[2W_{N+1}]&=\frac{Z_{N+1}(+,-)}{Z_{N+1}(-,+)}\ ,\end{aligned} \tag{4}$$

which, after a straightforward calculation, can be written as

$$\begin{aligned}X_{N+1}&=\frac{q+1}{2}\ln\left\{\frac{F_N^+(K)}{F_N^-(K)}\right\}\ ,\\ Y_{N+1}&=-\gamma K+\frac{q+1}{2}\ln\left\{\frac{G_N^+(K)}{F_N^-(K)}\right\}\ ,\\ W_{N+1}&=\frac{q+1}{2}\ln\left\{\frac{G_N^+(K)}{G_N^-(K)}\right\}\ ,\end{aligned} \tag{5}$$

where

$$F_N^{\pm}(K)=e^{\pm 2K+2X_N}+e^{2Y_N}+e^{2Y_N-2W_N}+e^{\mp 2K} \tag{6}$$

and

$$G_N^{\pm}(K)=e^{2X_N}+e^{\pm 2K+2Y_N}+e^{\mp 2K+2Y_N-2W_N}+1\ . \tag{7}$$

The recursion relations for the effective fields acting on successive generations are quite similar to Eq. (5), where the $q+1$ factor is to be replaced by q. Note that if the two layers are ferromagnetically coupled, we must have $\langle\sigma_0^1\rangle=\langle\sigma_0^2\rangle$, which implies that $W_N=0$ in the thermodynamic limit. Otherwise, when they are antiferromagnetically coupled, $\langle\sigma_0^1\rangle=-\langle\sigma_0^2\rangle$ and consequently $X_N=0$ as $N\to\infty$. Therefore, in both cases, we have effectively a system of two coupled recursion relations: one for a critical field related to the order parameter along each layer and another for a noncritical field associated with the interlayer spin-spin correlation function.

The transition line in the space of parameters T_c-γ between the ferromagnetic (F) and paramagnetic (P) phases for ferromagnetically coupled layers can be obtained by imposing that, at the transition, the critical field X^* goes continuously to zero in the thermodynamic limit. The assumption of an infinitesimal effective field at the boundary is required in order to provoke the appearance of nontrivial results.[15] After some manipulation we obtain the following expression for the critical line:

$$\exp(2\gamma K_c)=\frac{\cosh(2K_c)-\sinh(2K_c)/q}{q\sinh(2K_c)-\cosh(2K_c)}\ . \tag{8}$$

The phase diagram is depicted in Fig. 1 for the particular cases of $q=2$ and 100. Note that for $\gamma=0$ we recover the transition temperature of a single Bethe lattice, as expected. Otherwise, in the opposite limit of $\gamma\to\infty$, the transition temperature goes asymptotically to a value which is twice the one for uncoupled lattices, since the interlayer pairs become rigidly correlated. For $q+1=4$ and $\gamma=1.0$, the relation obtained between the transition temperatures of the bilayer and monolayer systems agrees qualitatively well with previous Monte Carlo and series-expansion results from coupled square lattices.[16] The slope of the transition line at $\gamma=0$ is given by

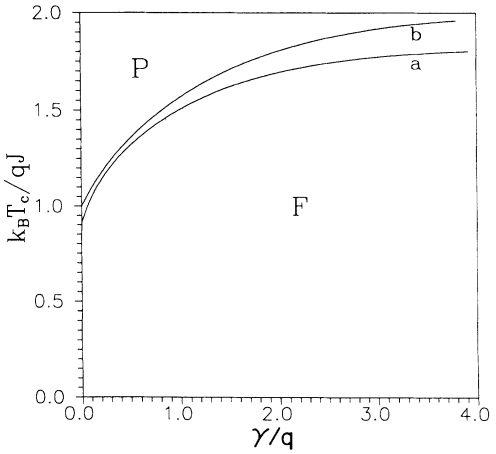

FIG. 1. Normalized transition temperature for two coupled Bethe lattices vs the coupling parameter γ for (a) $q=2$ and (b) $q=100$.

$$\zeta=\frac{d}{d\gamma}(k_B T_c/J)|_{\gamma=0}=\left\{\frac{1}{2}(q-1)\ln\left[\frac{q+1}{q-1}\right]\right\}^{-1}, \quad (9)$$

which decreases as the coordination number increases, with limits $\zeta(q=2)=2/\ln(3)$ and $\zeta(q\to\infty)=1.0$.

ANNEALED INTERLAYER BOND DISORDER

For an annealed distribution of bonds, the configurational average is done over the partition function. This is, for practical purposes, performed by introducing in the Hamiltonian a disorder variable n_i and a chemical potential per disordered bond, μ. For interlayer disordered bonds, the Hamiltonian can be written as

$$H=-J\sum_{i,j}(\sigma_i^1\sigma_j^1+\sigma_i^2\sigma_j^2)-J\sum_i\sigma_i^1\sigma_i^2[\gamma(1-n_i)+\gamma' n_i]-\mu\sum_i n_i , \quad (10)$$

where n_i takes the value 0 (1) if the bond has a coupling constant γJ ($\gamma' J$). Here the chemical potential associated with the annealed disorder is chosen so as to make the thermodynamic-averaged concentration of $\gamma' J$ couplings, that is, $\langle n_i\rangle$, temperature independent. Following the recipe introduced in the latter section, the recursion relations for the partial partition function are now given by

$$Z_{N+1}(\sigma_0^1,\sigma_0^2)=\sum_{n_0}\exp\{[\gamma(1-n_0)+\gamma' n_0]K\sigma_0^1\sigma_0^2+\Delta n_0\}\times\prod_{i=1}^{q+1}\sum_{\sigma_i^1,\sigma_i^2}\exp[K(\sigma_0^1\sigma_i^1+\sigma_0^2\sigma_i^2)]\times Z_n(\sigma_i^1,\sigma_i^2) , \quad (11)$$

where $\Delta=\mu/k_B T$. Defining the effective fields as in Eq. (4), the recursion relations for the critical fields X_{N+1} and W_{N+1} remain the same as in the pure coupled layers. For the noncritical field we now obtain

$$Y_{N+1}=\frac{q+1}{2}\ln\left\{\frac{H^+(K,\gamma,\gamma',\Delta)}{H^-(K,\gamma,\gamma',\Delta)}\right\}+\frac{q+1}{2}\ln\left\{\frac{G_N^+(K)}{F_N^-(K)}\right\}, \quad (12)$$

where

$$H^{\pm}(K,\gamma,\gamma',\Delta)=e^{\pm\gamma K+\Delta}+e^{\mp\gamma' K} . \quad (13)$$

Here, as before, to obtain the general recursion relation for successive effective fields, one must substitute the factor $q+1$ by q in Eq. (12). The chemical potential is eliminated in favor of the mean number of $\gamma' J$ bonds,

$$p=\langle n_0\rangle=\sum_{\sigma_0^1,\sigma_0^2}Z'_{N+1}(\sigma_0^1,\sigma_0^2)\Big/\sum_{\sigma_0^1,\sigma_0^2}Z_{N+1}(\sigma_0^1,\sigma_0^2) , \quad (14)$$

with

$$Z'_{N+1}(\sigma_0^1,\sigma_0^2)=\exp[\gamma' K\sigma_0^1\sigma_0^2+\Delta]\times\prod_{i=1}^{q+1}\sum_{\sigma_i^1,\sigma_1^2}\exp[K(\sigma_0^1\sigma_i^1+\sigma_0^2\sigma_i^2)]\times Z_N(\sigma_i^1,\sigma_i^2) , \quad (15)$$

which will be taken as an independent parameter. The phase diagram in the T_c-p plane for the particular case of $\gamma'=-\gamma$ is shown in Fig. 2 for a few values of γ. Note that for $p=\frac{1}{2}$ the lattices become decoupled. For concentrations of antiferromagnetic (AF) bonds in the range $p<\frac{1}{2}$, the net coupling between the layers is still ferromagnetic and they are ferromagnetically coupled, while for $p>\frac{1}{2}$ the resulting coupling is antiferromagnetic. In no way can annealed interlayer disorder destroy the intraplane long-range order.

ANNEALED INTRALAYER BOND DISORDER

The most interesting case is when there is disorder inside each layer. This is, for example, the case of doped high-T_c superconductors in which the holes introduced by doping are believed to be mainly localized in the oxygen sites of the CuO_2 sheets.[8] The holes induce an effective coupling between adjacent Cu ions[9] in such a way that one can consider each layer as containing a random bond distribution.[17] The statistical correlations between the bond distribution of each layer bring up interesting properties of the phase diagram, as we shall see below.

In this case the Hamiltonian can be put in the form

$$H=-J\sum_{i,j,l}[(1-n_j^l)+\alpha n_j^l]\sigma_i^l\sigma_j^l-\mu\sum_{j,l}n_j^l-\gamma J\sum_i\sigma_i^1\sigma_i^2 , \quad (16)$$

where n_j^l denotes the bond disorder variable for the bond

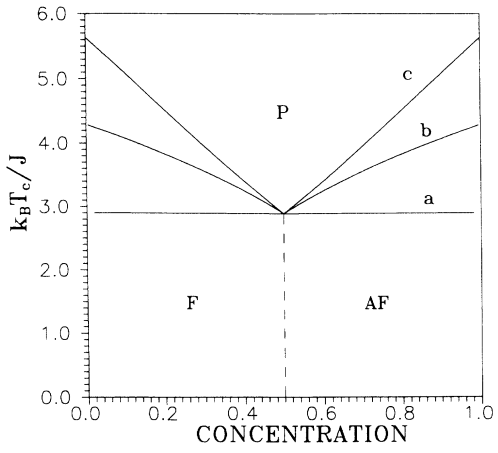

FIG. 2. Phase diagram in the T_c-p plane for coupled Bethe lattices with disordered interlayer couplings in the particular case of $\gamma'=-\gamma$, $q=3$, and (a) $\gamma=0.01$, (b) $\gamma=2.0$, and (c) $\gamma=10.0$. The dashed line separates the regions in which the layers are ferromagnetically and antiferromagnetically coupled.

that connects the site j to a site located at the previous generation $j-1$ at the layer l and takes the value 0 (1) as the coupling strength is J (αJ). Here $p=\langle n_j^l \rangle$ is the thermodynamic average of the concentration of coupling constants αJ of the intralayer bonds. A straightforward calculation using the recipe previously introduced leads to the following equations for the effective fields acting on the central pair:

$$X_{N+1}=\frac{q+1}{2}\ln\left\{\frac{F_N^+(A)}{F_N^-(A)}\right\},$$

$$Y_{N+1}=-\gamma K+\frac{q+1}{2}\ln\left\{\frac{G_N^+(A)}{F_N^-(A)}\right\}, \tag{17}$$

$$W_{N+1}=\frac{q+1}{2}\ln\left\{\frac{G_N^+(A)}{G_N^-(A)}\right\},$$

where

$$A=\frac{1}{2}\ln\left\{\frac{e^K+e^{\alpha K+\Delta}}{e^{-K}+e^{-\alpha K+\Delta}}\right\}, \tag{18}$$

and similar ones for successive effective fields substituting $q+1$ by q. The phase diagram can be readily obtained after one eliminates the chemical potential. Let us first analyze the case where we have coupled diluted layers ($\alpha=0$). In Fig. 3 we show the transition line in the T_c-p plane for the cases of uncoupled, weakly coupled, and strongly coupled layers. A general feature is that for two coupled layers the percolation concentration is distinct from the one in the monolayer limit and can be analytically obtained as

$$p_c^B(q,n=2)=\frac{q-1+(q^2-1)^{1/2}}{2q}, \tag{19}$$

which for $q=3$ gives $p_c^B(q=3,\ n=2)=0.8047\ldots$. Note that for completely random bond distributions, as, for example, in quenched disordered systems, the percolation threshold for two coupled Bethe lattices is $p_c=1-1/q^2$, yielding $p_c(q=3)=0.888\ldots$. The annealing induces correlations between bonds localized at different layers so that $1-1/q<p_c^B<1-1/q^2$, where $p_c^B(q,n=1)=1-1/q$ is the percolation concentration of a single Bethe lattice. The fact that $p_c^B(q=3,\ n=2)>1-1/q$ means that the induced correlation in this diluted limit is not enough to promote a one-to-one correspondence between parallel bonds, in which case the percolation concentration should be the same as that of a monolayer. A weak bond-bond correlation at the ground state of a randomly diluted Bethe lattice in the annealed regime has also been predicted,[18] but the percolation concentration is the same in both annealed and quenched regimes,[19] in contrast to the result for a bilayer.

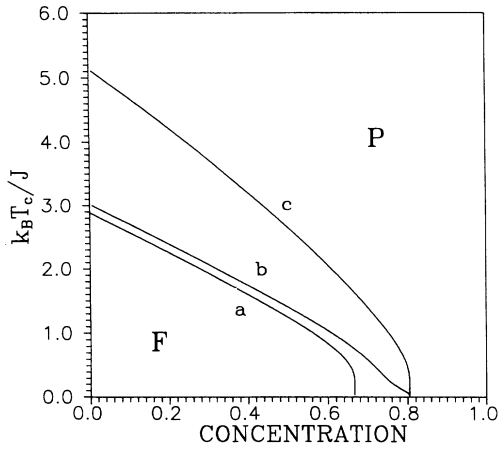

FIG. 3. Phase diagram in the T_c-p plane for coupled Bethe lattices with diluted intralayer bonds for $q=3$ and (a) $\gamma=0.0$, (b) $\gamma=0.1$, and (c) $\gamma=5.0$. Note that for weakly coupled layers there is a crossover from uncoupled to coupled regimes.

The percolation concentration for n-coupled layers with intralayer-annealed dilution can be straightforwardly obtained for some simple geometries by using the decoration transformation.[20] For n-coupled Bethe lattices, this procedure leads to

$$p_c^B(q,n)=\frac{q-1}{2q}\left[1+\left[\frac{q+1}{q-1}\right]^{1-1/n}\right], \tag{20}$$

while for n-coupled square lattices it gives

$$p_c^S(n)=\frac{1-\sqrt{2}/2}{2}[1+(\sqrt{2}+1)^{2-1/n}]. \tag{21}$$

Note that, although n-coupled Bethe lattices with coordination number $q+1=4$ have a large percolation threshold when compared with coupled square lattices [$p_c^S(n=2)=0.6957\ldots$, $p_c^S(n=3)=0.7827\ldots$, to compare with $p_c^B(q=3,\ n=2)=0.8047\ldots$, $p_c^B(q=3,\ n=3)=0.8624\ldots$], the above expressions have the same asymptotic behavior $p_c(\infty)-p_c(n)\propto n^{-1}$ as $n\to\infty$.

Let us now consider competing parameters ($\alpha<0$). In this case the induced interlayer correlation between parallel bonds in the ground state is so strong that it permits the distribution of antiferromagnetic bonds in each layer to be completely equivalent. This fact has the consequence that the critical concentration above which the long-range ferromagnetic order disappears is the same for coupled and uncoupled lattices. This behavior is well illustrated in Fig. 4, where the antiferromagnetic couplings are stronger than the ferromagnetic ones ($\alpha=-1.5$). The transition line for weakly coupled lattices presents a reentrant behavior, which can be understood by means of the following considerations: as the temperature increases, the one-to-one correspondence between parallel bonds is broken down and a large path composed only of ferromagnetic bonds can be performed by jumping from one layer to another. In this way, for a concentration just above the critical one in which the ground state is paramagnetic, an increase of temperature can stabilize a long-range order, as a result of the appearance of larger paths. This mechanism can be well illustrated through the analysis of the nearest-neighbor intralayer bond-bond and interlayer bond-bond and spin-spin correlation functions, which are, respectively, defined as

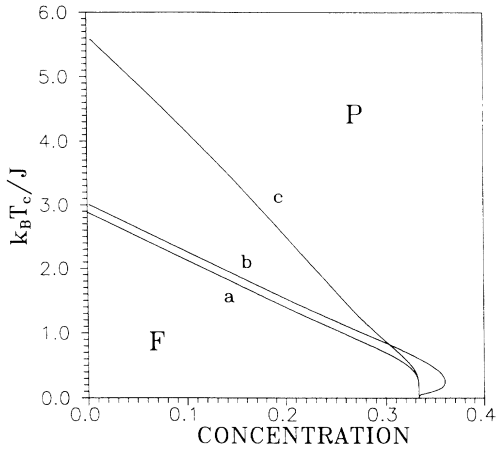

FIG. 4. Phase diagram in the T_c-p plane for coupled Bethe lattices with competing intralayer couplings for $q=3$, $\alpha=-1.5$, and (a) $\gamma=0.0$, (b) $\gamma=0.1$, and (c) $\gamma=10.0$. The reentrant behavior appears for weakly coupled layers. Note that the critical concentration is the same for uncoupled and coupled layers, contrary to the diluted case.

$$C(n_0^1,n_1^1)=(\langle n_0^1 n_1^1\rangle-p^2)/(p-p^2)\ , \tag{22}$$

$$C(n_0^1,n_0^2)=(\langle n_0^1 n_0^2\rangle-p^2)/(p-p^2)\ , \tag{23}$$

$$C(\sigma_0^1,\sigma_0^2)=\langle\sigma_0^1\sigma_0^2\rangle-\langle\sigma_0^1\rangle^2\ , \tag{24}$$

where these correlations are normalized in order to achieve the maximum value 1.0 in the regime of extreme correlations. In Fig. 5 we show the behavior of these correlations as a function of temperature for a set of parameters for which a reentrant phase diagram is predicted. At very low temperatures the interlayer correlations indicate that the two layers are rigidly coupled, as the spin and bond configurations are the same. In this way the bilayer behaves like a single layer that for this concentration of antiferromagnetic bonds has a paramagnetic ground state. As temperature increases, the interlayer bond-bond correlation decays faster than the interlayer spin-spin correlation. Therefore the appearance of a large ferromagnetically correlated cluster is favored in view of the fact that, while the one-to-one correspondence between parallel bonds fades away, the spin-spin correlations stay strong enough to transport the intralayer ferromagnetic short-range order from one layer to the other. Consequently, a transition to a long-ranged ferromagnetically ordered phase may take place by increasing the temperature. In the illustrated case this transition is detected by a discontinuous derivative of the intralayer bond-bond correlation. At higher temperatures the thermal fluctuations destroy the spin-spin correlations and the disordered phase becomes again the most stable. The interval between the two kinks in the intralayer bond-bond correlation function represents the range of temperatures in which the system is ferromagnetically ordered. For strongly coupled layers the coherence between the bond distributions is lost only at high temperatures. In this case such a mechanism does not succeed in inducing an ordered phase because of the presence of large thermal fluctuations and so no reentrance is observed. The two competing roles played by temperature, that is, the tendency to break intraplane spin-spin correlations destroying the long-range order and the break of interplane bond-bond correlation that makes possible the formation of large clusters, is actually the underlying mechanism that leads to the reentrance shown in Fig. 4.

If the antiferromagnetic couplings are weaker than the ferromagnetic ones ($-1<\alpha<0$), a reentrant behavior exists even in the uncoupled limit. This is due to the fact that the weak antiferromagnetic couplings are more sensitive to thermal fluctuations, and therefore the frustration effect induced by them is smoothed out by temperature. Again, there are two competing effects induced by thermal fluctuations: the breakdown of spin-spin correla-

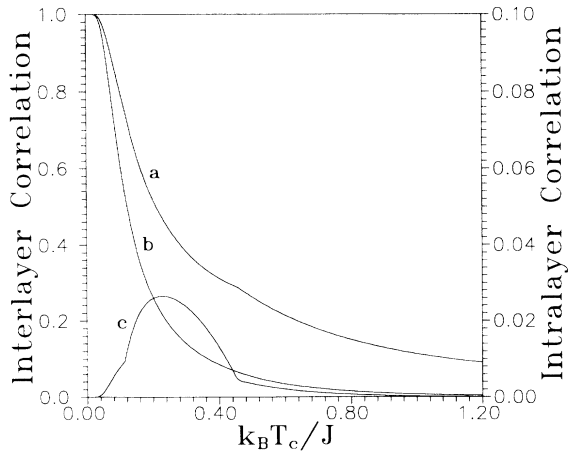

FIG. 5. (a) Interlayer spin-spin, (b) interlayer bond-bond, and (c) intralayer bond-bond nearest-neighbor correlations as a function of temperature for $q=3$, $p=0.35$, $\alpha=-1.5$, and $\gamma=0.1$. The two singularities in the intralayer bond-bond correlation are the signature of a reentrant phase diagram.

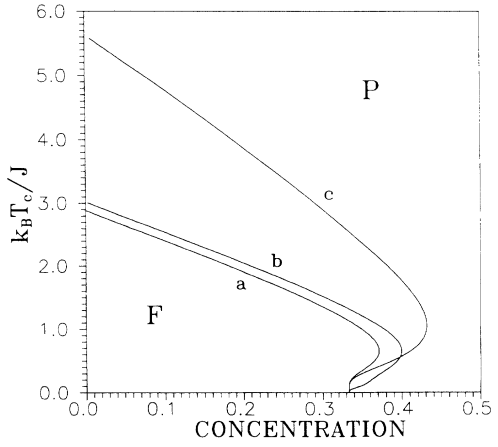

FIG. 6. Phase diagram in the T_c-p plane for coupled Bethe lattices with competing intralayer couplings for $q=3$, $\alpha=-0.5$, and (a) $\gamma=0.0$, (b) $\gamma=0.1$, and (c) $\gamma=10.0$. A reentrance appears even in the uncoupled case.

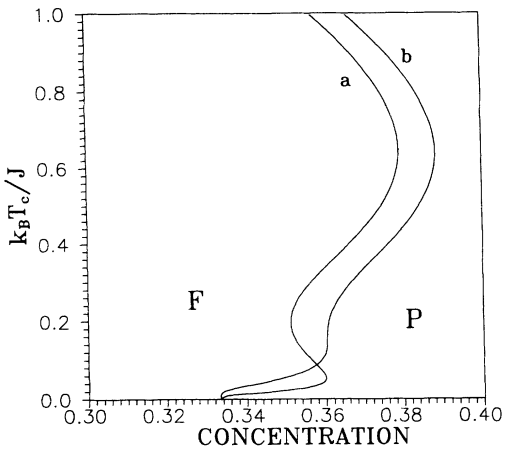

FIG. 7. Phase diagram in the T_c-p plane for weakly coupled Bethe lattices with competing couplings for $q=3$, $\alpha=-0.5$, and (a) $\gamma=0.02$ and (b) $\gamma=0.05$. A reentrant behavior appears with even four transition temperatures.

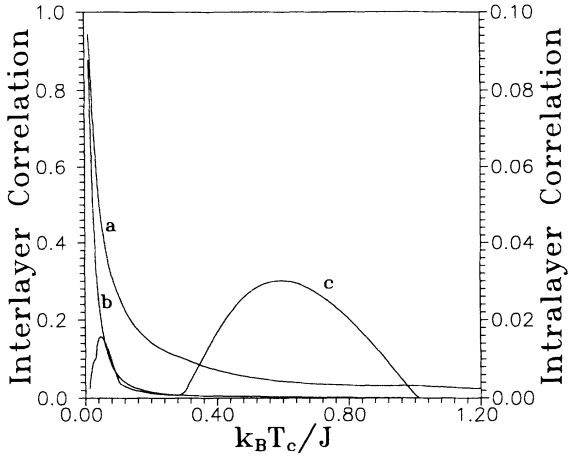

FIG. 8. (a) Interlayer spin-spin, (b) interlayer bond-bond, and (c) intralayer bond-bond nearest-neighbor correlations as a function of temperature for $q=3$, $p=0.35$, $\alpha=-0.5$, and $\gamma=0.02$. The first reentrance is due to the loss of coherence between the bond distributions and the second one to the smoothing out of the frustration effects in the monolayers.

tions and the smoothing out of the frustration effects. This competition represents a different mechanism for the appearance of a reentrance, which has been exhaustively discussed in the literature as a property inherent to the doped frustrated monolayer system.[19,21] When the lattices are coupled, the two mechanisms described above are present but superposed for almost all ranges of the interplane coupling parameter γ, as depicted in Fig. 6. The reentrances are separated only in the regime of very small interplane coupling, as shown in Fig. 7, where a multiple reentrance is observed with four transition temperatures in the particular ranges of concentration. In Fig. 8 the correlation functions [Eqs. (22)–(24)], in the regime where a multiple reentrance appears, clearly show that the first reentrance is due to the loss of coherence between the bond distribution. The second one is typical of the monolayer system since in this range of temperatures they are weakly correlated. In the present case this reentrance is due to the smoothing out of the frustration effects. The four singularities in the intralayer bond-bond distribution delimit the regions where the ferromagnetic order is stable. A similar phenomenon of multiple reentrance has been observed in liquid crystals,[22] whose origin is related to the intrinsic frustrated structure of monolayers.[23]

CONCLUSIONS

We have exactly obtained the phase diagrams of coupled bilayers composed of two interacting Bethe lattices with annealed intra- and interlayer bond disorder. It was observed that the lattices with small coordination number are more sensitive to coupling effects and that interlayer disorder cannot destroy the in-plane long-range order. In the limit of intralayer dilution, we have obtained a percolation concentration that is different from that expected for uncorrelated bond distribution. However, there is only a weak bond-bond interlayer correlation that still permits the growth of an infinite cluster even for concentrations of missing bonds above the single-lattice percolation threshold. In the case of competing disordered bonds, where frustration effects are present, the bond-bond correlation in the ground state is strong enough to promote a one-to-one correspondence between the adjacent layers so that the critical concentration, above which the ground state is disordered, is the same for coupled and uncoupled lattices. However, a very interesting phenomenon of multiple reentrance appears as a result of the relative influence played by thermal fluctuations on the frustration effects and on the spin-spin and bond-bond correlation functions. Similar correlation between disorder distribution has been observed in two coupled superconducting films, where a tendency to align the vortices, in the strong-coupling limit, has as a consequence the fact that the superconducting transition temperature remains the same of that of one thick film.[24] Furthermore, a reentrant disordered phase was recently reported in two-layer films of Kr on graphite, whose origin is suggested to be related to the loss of coherence between the first and second layers as T increases.[25] We also believe that the reentrance phenomenon observed in high-T_c superconductors[26] is based in the same mechanisms described in this work, but further analysis of the correlation functions is required to clarify this point.

ACKNOWLEDGMENTS

We thank Dr. Solange B. Cavalcanti, Dr. Sérgio G. Coutinho, and Dr. Roberto B. Muniz for fruitful discussions and their critical reading of the manuscript. This work was partially supported by Conselho Nacional de Desenvolvimento Científico e Tecnológico-CNPq and Financiadora de Estudos e Projetos-FINEP (Brazilian Research Agencies).

[1]See, e.g., S. D. Bader, Proc. IEEE **78**, 909 (1990), and references therein.

[2]W. Staecklin, S. S. P. Parkin, and J. C. Scott, Phys. Rev. B **39**, 6854 (1988).

[3]M. N. Baibich *et al.*, Phys. Rev. Lett. **61**, 2472 (1988); J. Unguris, R. J. Celotta, and D. T. Pierce, *ibid.* **67**, 140 (1991); S. S. P. Parkin, N. More, and K. P. Roche, *ibid.* **64**, 2304 (1990).

[4]A. Kueny *et al.*, Phys. Rev. B **29**, 2879 (1984); R. E. Camley, T. S. Rahman, and D. Mills, *ibid.* **27**, 261 (1983).

[5]M. E. Fisher and H. Nakanishi, J. Chem. Phys. **75**, 5857 (1981); A. M. Nemirovsky and K. F. Freed, J. Phys. A **18**, L319 (1985); H. T. Diep, Phys. Rev. B **43**, 8509 (1991); Q. Hong, *ibid.* **41**, 9621 (1991).

[6]B. Heinich *et al.*, Phys. Rev. B **38**, 12 879 (1988); Kh. M. Pashev and D. L. Mills, *ibid.* **43**, 1187 (1991).

[7]T. Wang *et al.*, Phys. Rev. B **43**, 8623 (1991); S. Hasegawa *et al.*, *ibid* **43**, 7631 (1991); R. A. Klemm and S. H. Liu, *ibid.* **44**, 7526 (1991). See also Refs. 10 and 11.

[8]T. R. Dinger *et al.*, Phys. Rev. Lett. **58**, 2687 (1987); T. K. Worthington, W. J. Gallagher, and T. R. Dinger, *ibid.* **59**, 1160 (1987); V. J. Emery, *ibid.* **58**, 2794 (1987).

[9]I. Morgenstern, Z. Phys. B **70**, 299 (1988); A. Aharony *et al.*, Phys. Rev. Lett. **60**, 1330 (1988).

[10]W. E. Pickett, Rev. Mod. Phys. **61**, 433 (1989).

[11]M. Gulacsi and Zs. Gulacsi, Phys. Rev. B **42**, 3981 (1990).

[12]See, e.g., J. Vannimenus, Z. Phys. B **43**, 141 (1981); C. S. Yokoi, M. J. de Oliveira, and S. R. Salinas, Phys. Rev. Lett. **54**, 163 (1985); D. J. Thouless, *ibid.* **56**, 1082 (1986); J. M. Carlson *et al.*, Europhys. Lett. **5**, 355 (1988).

[13]C. J. Thompson, J. Stat. Phys. **27**, 441 (1982); C. R. da Silva and S. Coutinho, Phys. Rev. B **34**, 7975 (1986).

[14]C. Kwon and D. J. Thouless, Phys. Rev. B **43**, 8379 (1991).

[15]S. Inawashiro, C. J. Thompson, and G. Honda, J. Stat. Phys. **33**, 419 (1983).

[16]K. Binder and P. C. Hohenberg, IEEE Trans. Magn. Magn. **MAG-12**, 66 (1976), and references therein.

[17]D. C. Mattis, Phys. Rev B **38**, 7061 (1988); R. J. V. dos Santos *et al.*, *ibid.* **40**, 4527 (1989); P. Paul and D. Mattis, *ibid.* **44**, 2384 (1991).

[18]M. L. Lyra and S. B. Cavalcanti, Phys. Rev. B **45**, 8021 (1992).

[19]M. L. Lyra and S. Coutinho, Physica A **155**, 232 (1989).

[20]I. Syozi, in *Phase Transitions and Critical Phenomena,* edited by C. Domb and M. S. Green (Academic, New York, 1972), Vol. 1.

[21]D. P. Landau, Phys. Rev. B **16**, 4164 (1977); T. E. Shirley, *ibid.* **16**, 4078 (1977); P. Shukla and M. Wortis, *ibid.* **21**, 159 (1980); K. De'Bell, J. Phys. C **13**, L651 (1980); R. J. V. dos Santos, F. C. S. Barreto, and S. Coutinho, J. Phys. A **23**, 2563 (1990).

[22]N. H. Tinh *et al.*, J. Phys. (Paris) **43**, 1127 (1982); F. Hardouin *et al.*, J. Chim. Phys. **80**, 53 (1983).

[23]A. N. Berker and J. S. Walker, Phys. Rev. Lett. **47**, 1469 (1981); J. O. Indekeu and A. N. Berker, Phys. Rev. A **33**, 1158 (1986).

[24]E. Yap and G. Bergmann, Solid State Commun. **78**, 245 (1991).

[25]R. F. Hainsey *et al.*, Phys. Rev. B **44**, 3365 (1991). A reentrant transition has also been observed in $CdCr_{2x}In_{2-x}Se_4$ thin films: M Lubecka and L. J. Maksymowicz, *ibid.* **44**, 10 106 (1991).

[26]Y. Yeshurum *et al.*, Phys. Rev. B **36**, 840 (1987).